Gian Paolo Fadini,[1,2] Lisa Menegazzo,[1,2] Mauro Rigato,[1] Valentina Scattolini,[1,2]
Nicol Poncina,[1,2] Andrea Bruttocao,[1] Stefano Ciciliot,[1,2] Fabio Mammano,[2,3]
Catalin Dacian Ciubotaru,[4] Enrico Brocco,[5] Maria Cristina Marescotti,[1]
Roberta Cappellari,[1] Giorgio Arrigoni,[6,7] Renato Millioni,[1,7]
Saula Vigili de Kreutzenberg,[1] Mattia Albiero,[1,2] and Angelo Avogaro[1,2]

NETosis Delays Diabetic Wound Healing in Mice and Humans

Diabetes 2016;65:1061–1071 | DOI: 10.2337/db15-0863

Upon activation, neutrophils undergo histone citrullination by protein arginine deiminase (PAD)4, exocytosis of chromatin and enzymes as neutrophil extracellular traps (NETs), and death. In diabetes, neutrophils are primed to release NETs and die by NETosis. Although this process is a defense against infection, NETosis can damage tissue. Therefore, we examined the effect of NETosis on the healing of diabetic foot ulcers (DFUs). Using proteomics, we found that NET components were enriched in nonhealing human DFUs. In an independent validation cohort, a high concentration of neutrophil elastase in the wound was associated with infection and a subsequent worsening of the ulcer. NET components (elastase, histones, neutrophil gelatinase-associated lipocalin, and proteinase-3) were elevated in the blood of patients with DFUs. Circulating elastase and proteinase-3 were associated with infection, and serum elastase predicted delayed healing. Neutrophils isolated from the blood of DFU patients showed an increased spontaneous NETosis but an impaired inducible NETosis. In mice, skin PAD4 activity was increased by diabetes, and FACS detection of histone citrullination, together with intravital microscopy, showed that NETosis occurred in the bed of excisional wounds. PAD4 inhibition by Cl-amidine reduced NETting neutrophils and rescued wound healing in diabetic mice. Cumulatively, these data suggest that NETosis delays DFU healing.

Wound healing is impaired in diabetes, and diabetic foot ulcers (DFUs) cause significant morbidity and mortality risks (1). A combination of neuropathy and vasculopathy promotes DFUs, but the cellular and molecular mechanisms that delay successful tissue healing in diabetes are not well understood (2). This lack of information precludes new therapeutic strategies beyond glucose control, revascularization, and traditional wound care.

Inflammation is a typical feature of the wound healing process, and neutrophils are recruited early to the wound bed (3). Although neutrophils are instrumental to the clearance of micro-organisms, neutrophil depletion accelerates wound healing in animal models (4). Local infection, which is common in DFU, triggers neutrophil activation and the release of neutrophil extracellular traps (NETs) composed of granular proteins/enzymes and nuclear material (DNA and histones complexed in chromatin) (5). NETs entrap and remove bacteria using a sticky extracellular network loaded with bactericidal proteins (6). After extruding nuclear material, neutrophils retain a transient multitasking activity and then die by NETosis (5). NETosis begins with the activation of peptidyl arginine deiminase (PAD)4, which then leads to histone citrullination, massive chromatin decondensation, and the nuclear localization of granular enzymes (e.g., elastase) driven by reactive oxygen species from NADPH oxidase (NOX) (NOX dependent) or the mitochondrial respiratory chain (NOX independent) (7). These events culminate in the extrusion of chromatin and granule content into the extracellular space (8). NETs constitute a natural response against infection; however, excess or deregulated NETosis can cause tissue damage (9,10). We recently reported that high glucose in vitro

[1]Department of Medicine, University of Padova, Padova, Italy
[2]Venetian Institute of Molecular Medicine, Padova, Italy
[3]Department of Physics and Astronomy, University of Padova, Padova, Italy
[4]Centro Nazionale per le Ricerche Institute of Neuroscience, Padova, Italy
[5]Foot and Ankle Clinic, Policlinico di Abano Terme, Abano Terme, Italy
[6]Department of Biomedical Sciences, University of Padova, Padova, Italy
[7]Proteomic Center of Padova, University of Padova, Padova, Italy

Corresponding author: Gian Paolo Fadini, gianpaolo.fadini@unipd.it.

Received 24 June 2015 and accepted 29 December 2015.

This article contains Supplementary Data online at http://diabetes.diabetesjournals.org/lookup/suppl/doi:10.2337/db15-0863/-/DC1.

F.M. is currently affiliated with the CNR Institute of Cell Biology and Neurobiology, Monterotondo, Italy.

L.M., M.R., and M.A. contributed equally as co–second authors.

and hyperglycemia in patients with diabetes increased the release of NETs and circulating markers of NETosis (11,12). Wong et al. (13) found that PAD4 is overexpressed in diabetes, and NETosis induction can be demonstrated in murine models of DFU. Remarkably, the inhibition of NETosis by PAD4 knockout or disruption of NETs with DNase-1 accelerated wound healing. Therefore, we set out to validate these preclinical findings using a novel mouse model and to establish the effect of NETosis on the delayed wound healing in patients with diabetes. We took advantage of our platform developed for the identification of new candidate biomarkers and therapeutic targets in diabetic wound healing (14). This platform was based on a proteomic analysis of wound biopsies obtained from a "discovery" cohort of patients with DFUs who were unequivocally categorized as rapidly healing (RH) or nonhealing (NH). Protein biomarkers that showed a differential abundance in NH versus RH patients were retested using an independent "validation" cohort of patients with DFUs. Here, this approach confirmed the enrichment of NET-associated proteins in NH wounds. The data gathered from NETosis biomarkers, the in vitro analysis of human neutrophils, and a murine model suggest that NETosis delays diabetic wound healing in mice and humans.

RESEARCH DESIGN AND METHODS

Proteomic Analysis

We previously developed and validated a proteomic platform for the identification of biomarkers and new molecular pathways related to diabetic wound healing (14). This platform required the proteomic characterization of tissue lysates obtained from wound biopsies in patients ("discovery cohort") with wound outcomes clearly defined as RH (n = 17) or NH (n = 11). The details of this protocol were previously published (14). Here, we reanalyzed the data to evaluate the differential abundance of proteins associated with NETs in NH versus RH wounds. We built a custom pathway of NET-associated proteins. To validate the measurement of NET-associated proteins in individual wound lysates, we used samples collected from a validation cohort. Based on the wound outcome at follow-up, patients were divided into two groups: worsening ulcers or stable/healed ulcers.

Patients

The protocol was approved by the ethics committee of the University Hospital of Padova, and participants provided their informed consent. Three groups of individuals were enrolled: control subjects without diabetes, patients with diabetes, and patients with DFUs. Patients with DFUs underwent digital photographic documentation of the wound. The wound was classified according to perfusion, extent, depth, infection, and sensation (PEDIS) (15) and Texas University Classification (TUC) (16). For all participants, we collected data on demographics, anthropometrics, risk factors, diabetes complications, and medications. DFUs were classified as neuropathic, ischemic, or neuroischemic. Patients were followed under routine ambulatory care for wound treatment. We recorded the following events related to wound healing: complete healing, partial healing, worsening (defined as an increase in PEDIS/TUC compared with baseline), major/minor amputations, and revascularization.

Circulating Markers of NETosis

Histones were measured using the Cell Death Detection ELISAPLUS (Roche Diagnostics). The cell-free double-stranded DNA (dsDNA) was measured after phenol extraction using the Qubit 2.0 Fluorometer (Life Technologies). Elastase, neutrophil gelatinase-associated lipocalin (NGAL), lactoferrin, and proteinase-3 concentrations were measured using commercially available ELISA kits.

Human Neutrophils

Neutrophils were isolated using a nonactivating immunomagnetic cell-sorting technique (MACSxpress Human Neutrophil Isolation kit, Miltenyi Biotec). For stimulation of NOX-dependent NETosis, neutrophils were incubated with phorbol 12-myristate-13-acetate (PMA). For stimulation of NOX-independent NETosis, neutrophils were incubated with calcium ionophores, including a23187 and ionomycin. After 2 h of incubation, the cells were fixed with paraformaldehyde for immunofluorescence staining with anti-human PL2-3 monoclonal antibody (directed against the subnucleosomal complex of histones H2A and H2B and chromatin), anti-human neutrophil elastase, anti-human citrullinated (R2+R8+R17) histone H3, and Hoechst 33342. NETting cells were semiautomatically identified by comparing the fluorescence signals of the anti-chromatin antibodies to the Hoechst 33342 signal (17). In separate experiments, we used Cayman NETosis assays to determine the activities of NET-bound neutrophil elastase and myeloperoxidase (MPO).

Animals

All of the procedures were approved by the local ethics committee and the Italian Ministry of Health and conducted according to the National Institutes of Health Principles of Laboratory Animal Care. C57Bl/6J mice were used. Diabetes was induced with a single intraperitoneal injection of streptozotocin. For PAD4 inhibition, 10 mg/kg s.c. Cl-amidine was injected daily for 1 week prior to the generation of 4-mm excisional wounds. This daily treatment continued throughout the healing process.

For isolation of skin neutrophils, animals were killed, and the wound with a surrounding portion of skin was excised. The tissue was minced and digested in trypsin EDTA and collagenase type II, and the suspension was filtered. The cells were centrifuged, and the pellet was suspended in PBS for flow cytometry analysis. Bone marrow neutrophils were isolated according to the method outlined by Swamydas and Lionakis (18). The Sytox green assay was used to detect the release of NETs by cultured neutrophils stimulated with PMA or ionomycin.

Flow Cytometry

Mouse cells were stained with a monoclonal anti-mouse Ly-6C/G-PE (Gr-1) and 7-aminoactinomycin D. After washing with PBS, the cells were fixed with 2% paraformaldehyde

for 12 min at 37°C, washed with PBS, and then permeabilized with 90% methanol for 30 min at 4°C. Next, the cells were incubated with rabbit anti–histone H3 citrulline and rabbit anti–histone H4 citrulline antibodies for 30 min at 4°C. The cells were then incubated with an Alexa Fluor 488–conjugated goat anti-rabbit secondary antibody for 30 min at 4°C. The data were acquired using a FACS Canto instrument and analyzed with FlowJo X.

PAD4 Activity

PAD4 activity in lithium-heparin plasma and skin extracts was assessed with a commercially available kit (Cayman Chemicals). PAD4 activity was normalized based on the protein concentration measured with a bicinchoninic acid–based kit used according to the manufacturer's instructions.

Multiphoton Microscopy

Intravital Microscopy

Wild-type C57BL/6J mice were sedated with zolazepam/thylamine and xylazine, placed on a custom-made holder, and positioned under an Olympus ×25 objective. Wounds were evaluated at day 3. Thirty minutes before imaging, mice were injected with 5 μL i.v. Sytox green, 3 μL i.v. phycoerythrin-conjugated anti-mouse Gr-1, and 50 μL i.v. Hoechst 33342. In separate experiments, the vasculature of mice was stained by injecting 50 μL of a 10 mg/dL solution of high–molecular weight (150 kDa) fluorescein isothiocyanate–conjugated Dextran via the tail vein.

In Vitro

Neutrophils were immunomagnetically isolated from peripheral blood. For induction of the formation of NETs, neutrophils were stimulated with 100 nmol/L PMA at 37°C and 5% CO_2 for 2 h. Cells were stained with Hoechst 33342 (1:1,000 dilution from a 1 mg/mL solution) and 50 nmol/L tetramethylrhodamine (TMRM). Immediately prior to imaging, 100 nmol/L Sytox green was added to the media to allow for the visualization of extracellular dsDNA in NETs. The experiments were performed with an Olympus ×60 objective.

For all of the experiments, we used a modular multiphoton microscope (Bergano-II, Thorlabs) coupled with two synchronized pulsed laser beams. Two-photon microscopy at 800 nm excitation was used to visualize Sytox green and phycoerythrin-conjugated anti–Gr-1 monoclonal antibody, while three-photon excitation at 800 nm was used for Hoechst 33342 visualization.

See the Supplementary Data for additional details.

Statistical Analysis

The data are expressed as the mean ± SE or as a percentage. Normality was checked using the Kolmogorov-Smirnov test. Nonnormal variables were log transformed before statistical analysis. The comparisons of continuous variables between two or more groups were performed using Student *t* test or ANOVA. A post hoc least significant difference test was used. The comparisons of categorical variables between two or more groups were performed using the χ^2 test. A multivariable logistic regression analysis was used to evaluate the association between NETosis biomarkers and wound healing independent of confounding factors. Differences in survival curves were checked using the Gehan-Breslow-Wilcoxon test. Statistical significance was accepted at $P < 0.05$, and SPSS, version 22.0, was used to analyze the data.

RESULTS

NH Diabetic Wounds Contain Excess NET Components

We recently established a platform for the discovery and validation of novel biomarkers for tissue healing in patients with DFUs (14). We identified several proteins differentially expressed in RH versus NH diabetic wounds from a biopsy of the wound margin using tissue digestion, protein extraction, and proteomic analysis (14). The DAVID bioinformatic resource for functional annotation of genes/proteins revealed that proteins enriched in NH versus RH wounds belonged to "cell death," "protease activity," and "defense response" pathways (14). NETosis is a type of cell death that is associated with protease activation and triggered by infection. Therefore, functional annotations associated with NH wound features can be easily linked to NETosis. To build a custom "NETosis" pathway that is not preloaded on functional annotation tools, we screened the literature for articles with a detailed characterization of NET proteins. We identified 25 proteins that belonged to five subcellular compartments (nucleus, granules, cytoplasm/cytoskeleton, enzymes, and plasma membrane). These proteins were entered into a custom pathway (Fig. 1*A* and *B*). The expression of granular and nuclear NET components were 2.6- and 2.2-fold higher in NH versus RH wounds, respectively ($P < 10^{-6}$ and $P = 0.002$, respectively). Nongranular enzymes were mildly (1.3-fold) but significantly ($P < 10^{-4}$) enriched in NH versus RH wounds, whereas proteins of the cytoplasm, cytoskeleton, and plasma membrane were not significantly different between the two groups (Fig. 1*B* and *C*). According to a Gene Set Enrichment Analysis (GSEA) heat map, the custom NETosis pathway was enriched in NH versus RH wounds (Fig. 1*D*). These data indicate that typical granular and nuclear constituents of NETs are increased in the tissue lysates of NH diabetic wounds.

Elastase Content in Diabetic Wounds Is Associated With Impaired Healing

We quantified NET components (dsDNA, oligo- and mononucleosomes, and neutrophil elastase) in the tissue extracts of wound biopsies taken from an independent validation cohort of patients with DFUs (Table 1). Patients were divided into two groups based on the wound outcome at a 6-month follow-up: worsening wounds (n = 12) and healed or stabilized wounds (n = 33). For technical reasons, dsDNA and nucleosome measurements in frozen samples were not successful (data not shown). Neutrophil elastase, the prototypical NET marker, was 59% higher in worsening wounds compared with wounds

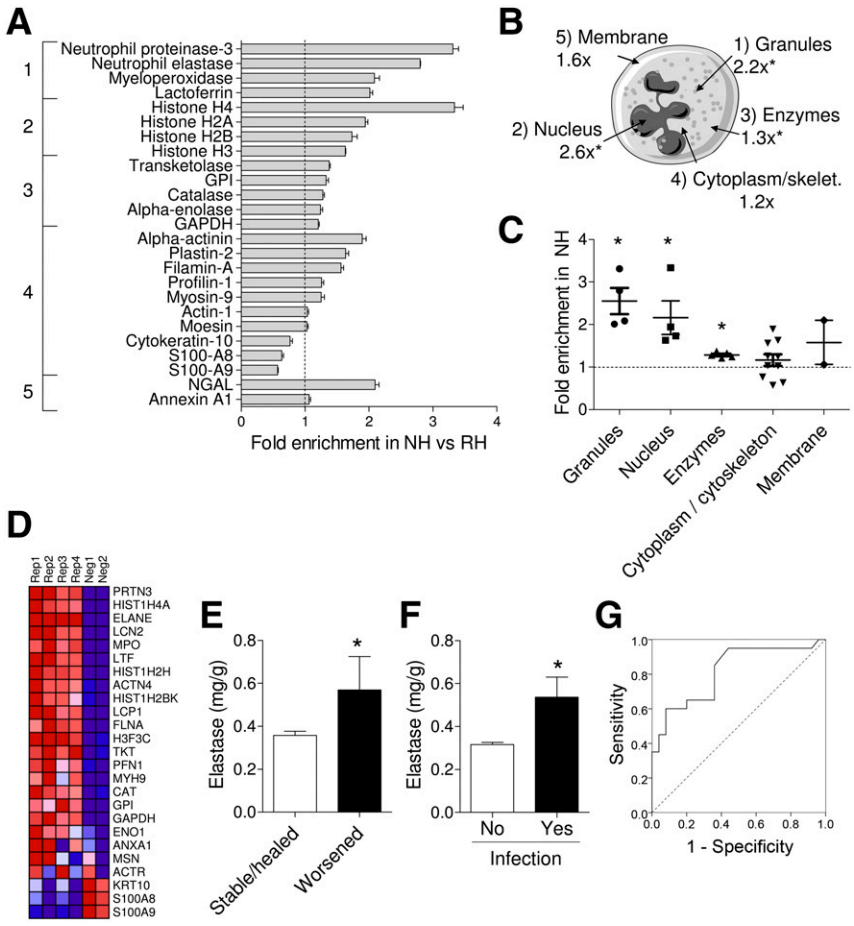

Figure 1—Proteomic analysis of diabetic wound lysates. *A*: Proteins belonging to the custom NETosis pathway are shown with their fold enrichment in NH vs. RH wounds. Error bars were derived from internal technical triplicates of the iTRAQ labels. The dashed line at onefold change aids visual identification of proteins with significant enrichment or depletion in NH vs. RH. Numbers on the left identify the belonging cellular compartment illustrated in *B*. *B*: Average fold enrichment for proteins in each subcellular compartment in NH vs. RH of proteins in the custom NETosis pathway (*$P < 0.05$). skelet., cytoskeleton. *C*: Fold enrichment in NH vs. RH with dispersion shown by individual dots of NETosis pathway proteins grouped according to subcellular compartment (*$P < 0.05$ compared with 1.0). *D*: Profile plot from the GSEA showing highly significant enrichment of most proteins in the custom NETosis pathway in the 4 replicates (Rep1–Rep4) compared with negative control subjects (Neg1, Neg2). False discovery rate–adjusted *P* value for this analysis, according to GSEA output, was <0.001, and normalized enrichment score was 2.06. *E*: Wound elastase content (measured as mg elastase/g tissue) in patients of the validation cohort showing stable/healed wounds vs. in those showing worsening wound evolution (*$P < 0.05$). *F*: Wound elastase content in patients of the validation cohort with and without microbiologically proven infection (*$P < 0.05$). *G*: Receiver operating characteristic curve showing the accuracy of wound elastase content in discriminating presence/absence of infection.

that were stable or healed ($P = 0.03$). These data suggest that local NETosis is associated with impaired wound healing (Fig. 1*E*). Infected wounds (20 of 45) had a 76% higher elastase content compared with noninfected wounds ($P = 0.012$) (Fig. 1*F*). Based on the receiver operating characteristic curve, elastase quantification showed a high accuracy for identifying the presence of infection (area under the curve 0.815 [95% CI 0.686–0.944]) (Fig. 1*G*).

Circulating NETosis Biomarkers Were Identified in Patients with DFUs

Diabetic foot syndrome is associated with systemic inflammation, and NET-associated biomarkers are locally increased in NH wounds. Thus, we determined whether NETosis biomarkers are increased in the bloodstream of patients with DFUs ($n = 52$) compared with matched patients with diabetes without DFUs ($n = 26$) and matched control subjects without diabetes ($n = 26$). In addition to dsDNA, we measured the NET components identified by a proteomic analysis, including histones, elastase, NGAL, proteinase-3, and lactoferrin. The clinical characteristics of the participants are shown in Table 1. Most DFU patients showed signs of systemic inflammation, with an elevated serum C-reactive protein concentration (median 71 mg/dL [interquartile range 16–123]), and 23% of DFU patients had mild leukocytosis (>11,000/μL). DFUs were classified as neuropathic, ischemic, or neuroischemic in 30.8%, 19.2%, and 50% of cases, respectively.

On average, the circulating levels of oligo- and mononucleosomes, neutrophil elastase, NGAL, and proteinase-3

Table 1—Clinical characteristics of patients in the validation cohort (study of local NETosis), divided according to wound outcome (no significant differences), and of patients in the study of systemic NETosis

	Study of local NETosis			Study of systemic NETosis		
	All	Stable/improved	Worsened	Controls	Diabetes	DFU
Number	45	33	12	26	26	52
Age, years	63.7 ± 1.4	64.4 ± 1.5	61.9 ± 3.14	70.6 ± 1.7	70.0 ± 1.3	70.8 ± 1.3
Male sex, %	95.6	93.9	100.0	53.8	53.8	65.4
BMI, kg/m^2	30.7 ± 0.8	30.9 ± 1.0	30.1 ± 1.6	25.8 ± 0.8	27.2 ± 0.8	31.4 ± 0.7*
HbA_{1c}, % (mmol/mol)	7.6 ± 0.3 (60 ± 2)	7.7 ± 0.3 (61 ± 2)	7.2 ± 0.7 (55 ± 5)	5.5 ± 0.1 (37 ± 1)	7.1 ± 0.2* (54 ± 2)	8.0 ± 0.2* (64 ± 2)
Diabetes duration, years	16.7 ± 1.8	16.7 ± 2.1	16.6 ± 3.6	—	10.2 ± 1.7	15.2 ± 1.4
Hypertension, %	73.3	69.7	83.3	61.5	73.1	94.2
Dyslipidemia, %	45.5	42.4	50.0	38.5	76.9	64.7*
Active smoking, %	30.9	30.3	25.0	30.8	38.4	22.4
Complications, %						
Coronary artery disease	27.2	30.3	16.7	7.7	7.7	28.8*†
Peripheral arterial disease	64.4	66.7	58.3	15.4	3.8	57.7*†
Retinopathy	43.5	36.4	41.7	0.0	19.2	64.7†
Neuropathy	78.6	69.7	83.3	0.0	11.6	51.9†
Chronic kidney disease	11.6	9.1	16.7	7.7	30.8	44.2*
Wound type, %						
Neuropathic	31.1	27.2	41.7	—	—	32.7
Ischemic	15.6	12.1	25.0	—	—	21.3
Neuroischemic	53.3	60.7	33.3	—	—	50.0
Medications, %						
Insulin	66.7	60.6	83.3	0.0	26.7	61.5†
Secretagogues	24.4	30.3	8.3	0.0	38.4	11.5
Metformin	28.9	33.3	16.7	0.0	73.1	36.5†
Incretins	0.0	0.0	0.0	0.0	19.2	3.8
Antiplatelet	65.1	66.7	63.6	46.2	46.2	57.7
Statin	38.6	30.3	58.3	23.1	80.8*	40.4†
ACE inhibitor/ARB	66.7	66.7	66.7	46.2	69.2	40.4
Other blood pressure–lowering	33.3	36.4	25.0	48.1	50.0	48.1

*$P < 0.05$ vs. control subjects. †$P < 0.05$ vs. patients with diabetes. ARB, angiotensin receptor blocker.

were significantly higher in DFU patients compared with patients with diabetes without DFUs and patients without diabetes (Fig. 2*A*, *B*, *D*, and *E*). The circulating level of cell-free dsDNA was not significantly increased in patients with DFUs, and the concentration of lactoferrin was not associated with diabetes or DFU (Fig. 2*C* and *F*). No differences in circulating NETosis biomarkers were detected among wound types (neuropathic, ischemic, or neuroischemic). A total of 59.6% of patients had a microbiologically proven infection, caused by Gram-positive bacteria in 60.7% of cases (mainly *Staphylococcus aureus*). *S. aureus* produces DNase, which may explain why dsDNA was not significantly increased in the bloodstream of DFU patients. In patients with microbiologically proven infections, neutrophil elastase was 41% higher compared with patients without wound infections ($P < 0.00$) (Fig. 2*G*). According to the PEDIS classification, there was a progressive rise in neutrophil elastase concentrations as the degree of infection worsened (Fig. 2*H*). Patients with Gram-positive bacterial infections had significantly higher elastase concentrations compared with patients with Gram-negative bacterial infections (Fig. 2*I*). The infection of DFU was associated with a 55% higher proteinase-3 concentration that progressively increased with the PEDIS infection score (Fig. 2*J* and *K*). Proteinase-3 levels tended to be higher in patients with polymicrobial infections compared with patients with unimicrobial infections (Fig. 2*L*). Circulating nucleosomes, dsDNA, and NGAL levels were not associated with infection (data not shown). Proteinase-3 is an auto-antigen in systemic vasculitis. Thus, we measured the level of antineutrophil cytoplasmic antibodies. The antineutrophil cytoplasmic antibody levels were very low in all of the patient groups (data not shown). PAD4 can be released in the extracellular space to catalyze the citrullination of autoantigen proteins (19). However, serum PAD4 activity was almost undetectable in all of the patient groups (data not shown). These negative findings indicate that NETosis plays different roles in DFUs and autoimmune disorders.

Circulating Biomarkers of NETosis and Wound Healing

Patients were followed for an average of 4.5 months. Complete wound healing occurred in 53.8% of patients,

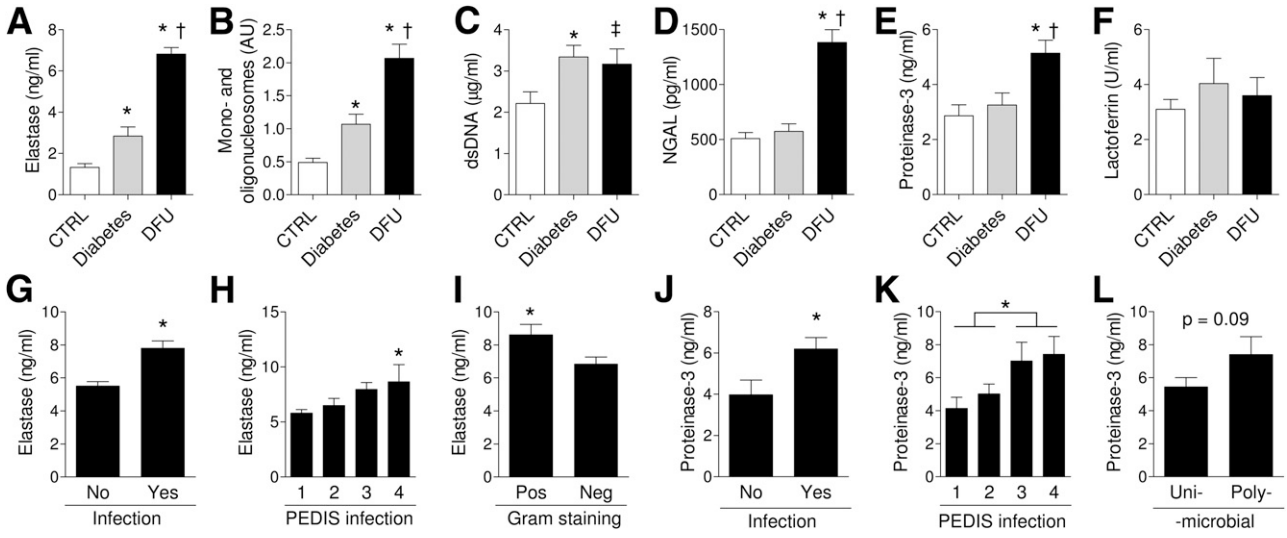

Figure 2—Circulating NETosis biomarkers in patients with DFU. *A–F*: Serum neutrophil elastase (*A*), mono- and oligonucleosomes (*B*), cell-free dsDNA (*C*), NGAL (*D*), proteinase-3 (*E*), and lactoferrin (*F*) concentrations in participants without diabetes (CTRL), with diabetes (Diabetes), and with DFU (post-ANOVA **P* < 0.05 vs. CTRL; †*P* < 0.05 vs. Diabetes; ‡*P* = 0.07 vs. CTRL). *G–I*: Serum neutrophil elastase concentrations in relation to presence/absence of microbiologically proven infection (**P* < 0.05 [*G*]), degree of infection according to the PEDIS classification (1, no symptoms/signs; 2, inflammation of the skin or subcutaneous tissue only; 3, extensive deeper erythema; 4, systemic inflammation response syndrome; **P* < 0.05 grade 4 vs. grade 1; *P* for trend <0.05 [*H*]) and infection by Gram-positive or -negative bacteria (**P* < 0.05 [*I*]). *J–L*: Serum proteinase-3 concentrations in relation to presence/absence of microbiologically proven infection (**P* < 0.05 [*J*]), degree of infection according to the PEDIS classification (**P* < 0.05 comparing degrees 3 and 4 with degrees 1 and 2 [*K*]), and in relation to the presence of polymicrobial vs. monomicrobial infection (*L*). AU, arbitrary units; Neg, negative; Pos, positive.

partial healing in 17.3%, and worsening in 5.7%; minor amputation occurred in 15.4% of patients, and major amputation in 9.6%; and revascularization occurred in 28.9% of patients. Spontaneous healing without amputation or revascularization occurred in 36.5% of patients. Serum neutrophil elastase was significantly lower in patients with completely healed wounds compared with patients with NH wounds and showed a tendency to decrease in patients with spontaneous healing (Fig. 3*A*). A logistic regression analysis showed that serum elastase was significantly inversely associated with complete healing ($P = 0.046$) after adjustment for infection and

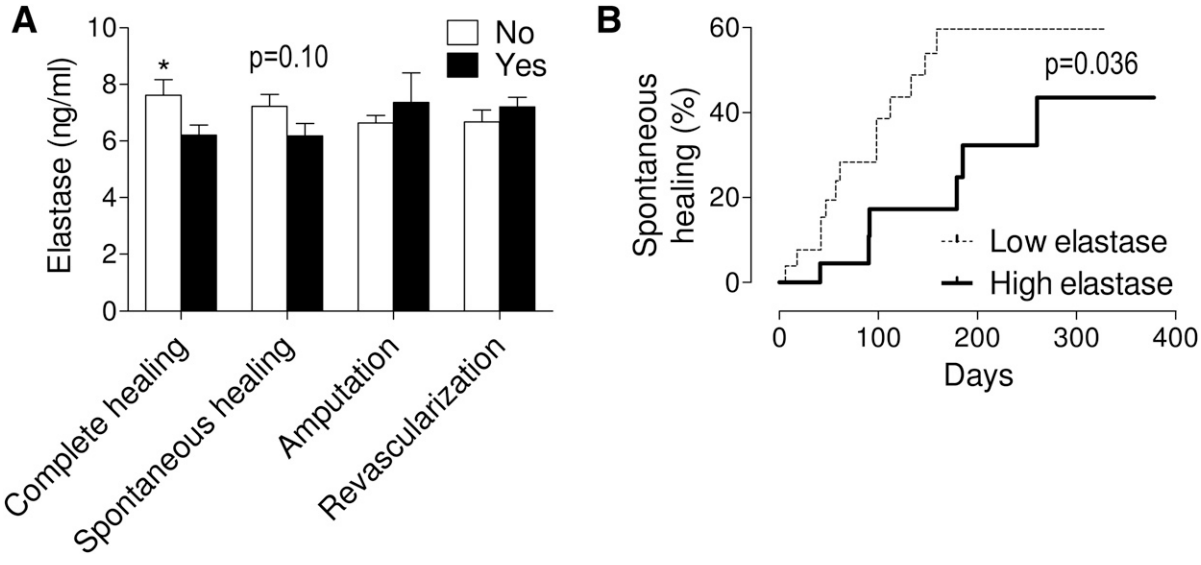

Figure 3—Circulating elastase and wound outcomes. *A*: Serum elastase concentrations are plotted in relation to wound outcomes (**P* < 0.05). Spontaneous healing was defined as complete healing without amputation or revascularization. Minor and major amputations are herein pooled. *B*: Kaplan-Meier curves showing the probability of spontaneous healing in patients categorized as having low (below-median) or high (above-median) serum elastase concentrations.

ischemia. According to the Kaplan-Meier curves, the probability of spontaneous healing over time was higher in patients with below-median elastase concentrations (P = 0.036) (Fig. 3*B*). Wound outcomes were not associated with nucleosome, dsDNA, NGAL, proteinase-3, or lactoferrin concentrations (data not shown).

Neutrophils From DFU Patients Are Primed to Undergo NETosis

DFU patients had elevated circulating NET components. Thus, we assessed whether the neutrophils of DFU patients were primed toward NETosis. We purified neutrophils using nonactivating immunomagnetic cell sorting and then evaluated spontaneous, NOX-dependent, and NOX-independent NETosis by incubating cells with PMA and the calcium ionophore a23187, respectively. We validated the induction of NETosis with PMA using immunofluorescence labeling of the nucleus, citrullinated histone H3, chromatin, and neutrophil elastase. A single-cell morphometric analysis revealed that a fraction of neutrophils incubated with PMA undergo chromatin decondensation and histone citrullination (Fig. 4*A*). NETs were visible as bead-on-a-string filaments after staining for chromatin and elastase (Fig. 4*B*). Transmission electron microscopy showed NETting neutrophils with loss of nuclear lobulation and extrusion of decondensed chromatin (Fig. 4*C*). Although these morphological aspects confirm the induction of NETosis in vitro, they exhibit high variability in quantitative analyses. Therefore, to estimate NET release, we used quantitative assays for DNA-bound neutrophil elastase and MPO, two NET proteins enriched in patients with diabetes with NH wounds. The elastase and MPO assays revealed a significant increase in the number of neutrophils primed for spontaneous NETosis in DFU patients (Fig. 4*D* and *E*). The NOX-dependent release of DNA-bound MPO but not elastase was increased in patients with diabetes regardless of DFU (Fig. 4*F* and *G*). The NOX-independent release of elastase and MPO in NETs was lower in patients with diabetes with control subjects (Fig. 4*H* and *I*). Based on the differences in basal NETosis levels, we calculated the fold induction of NOX-dependent and NOX-independent NETosis compared with the basal NETosis level for each group. There was a defect in NOX-dependent (for MPO) and NOX-independent (for both elastase and MPO) NETosis in patients with DFUs (Fig. 4*I* and *J*). These data indicate that DFUs prime neutrophils for spontaneous NETosis and compromise inducible NETosis.

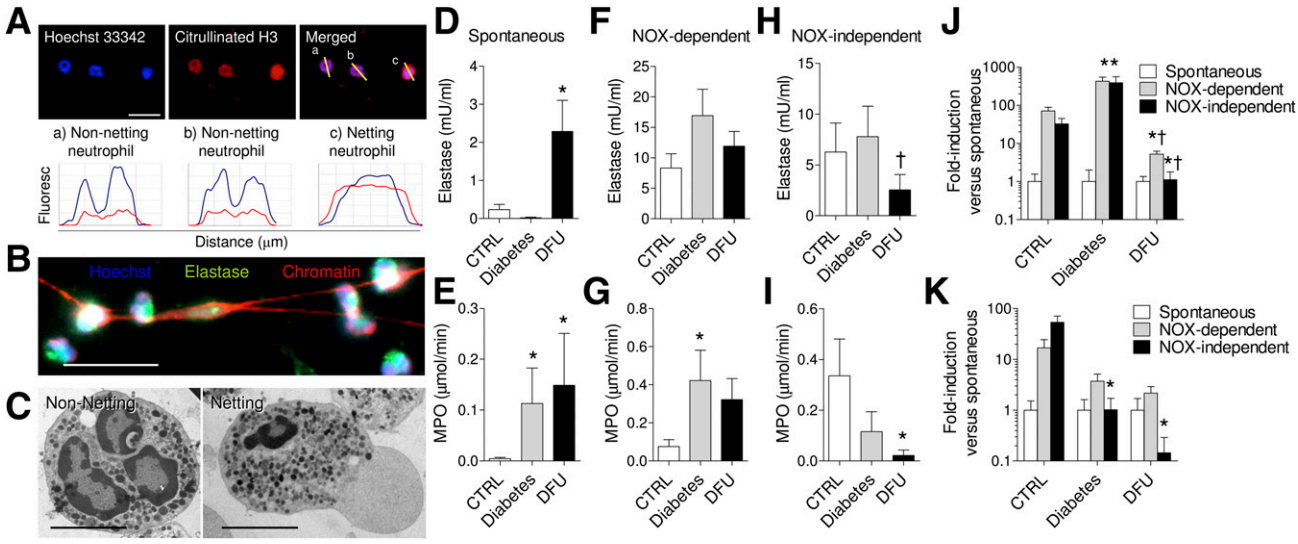

Figure 4—Analysis of NETosis in vitro. *A*: Single-cell morphometric analysis of neutrophils stimulated with PMA for 2 h and stained in blue with Hoechst 33342 to visualize the nuclear shape (the intercalating H33342 staining intensity is proportional to DNA concentration and thus declines with chromatin decondensation) and in red for citrullinated histone H3. Two non-NETting neutrophils and one NETting neutrophil are shown (scale bar 50 μm). The morphometric plots below report fluorescence (Fluoresc) intensity of the blue and red channels. In neutrophils undergoing NETosis, citrullinated histones spread out of the nuclear shape with decondensed chromatin. *B*: Visualization of NETs in a culture of neutrophils stimulated with PMA for 2 h and stained with H33342, elastase, and chromatin (scale bar 50 μm). *C*: Transmission electron microscopy showing a non-NETting neutrophil with normal morphology (left) and a NETting neutrophil with loss of nuclear polylobulation and extrusion of decondensed chromatin (right, scale bar 5 μm). *D–I*: Release of NET DNA-bound elastase (*D*, *F*, and *H*) and MPO (*E*, *G*, and *I*) by neutrophils purified from peripheral blood of participants without diabetes (CTRL), with diabetes (Diabetes), and with DFU under spontaneous NETosis (*D* and *E*); NOX-dependent NETosis stimulated by PMA (*F* and *G*); and NOX-independent NETosis stimulated by the calcium ionophore a23187 (*H* and *I*). Post-ANOVA: *P < 0.05 vs. CTRL; †P < 0.05 vs. patients with diabetes. *J*: Fold induction release of DNA-bound elastase by neutrophils in the three groups of patients with respect to spontaneous NETosis (*P < 0.05 vs. control subjects; †P < 0.05 vs. patients with diabetes). *K*: Fold induction release of DNA-bound MPO by neutrophils in the three groups of patients with respect to spontaneous NETosis (*P < 0.05 vs. control subjects).

NETosis Occurs in the Wound Bed

Wounds (4 mm in diameter) were created on the dorsal surface of the hind limb in mice with streptozotocin-induced diabetes. The analysis of tissue lysates by flow cytometry showed that wounded skin contained large amounts of Gr-1$^+$ neutrophils compared with intact skin; furthermore, the intracellular content of citrullinated histones H3/4 revealed that up to 10% of Gr-1$^+$ neutrophils were undergoing NETosis (Fig. 5*A* and *B*). With use of multiphoton confocal intravital microscopy, Gr-1$^+$ neutrophils were very rarely detected in the extravascular space of unwounded skin (Fig. 5*C*), whereas these cells abundantly infiltrated the skin 3 days after wounding (Fig. 5*D*). Typical NETosis markers were visible in the wound bed. During live imaging, putative NETting neutrophils were identified as Gr-1$^+$ cells devoid of nuclear staining or cells with massively delobulated nuclei with decondensed chromatin (low Hoechst signal). The NETting neutrophils were in close contact with extracellular dsDNA stained by Sytox green (Fig. 5*E*). We found NETosis features in vitro akin to those observed in vivo, including nuclear delobulation, chromatin decondensation, and dsDNA release (Fig. 5*F* and Supplementary Video 1). These data indicate that skin wounds promote the NETosis of infiltrating neutrophils.

Inhibition of NETosis Rescues Wound Healing in Diabetic Mice

NETosis is associated with the NH features of DFUs in patients, and it occurs within murine wounds. Thus, we tested the mechanistic ability of NETosis to delay wound healing. We blocked NETosis with the pharmacological PAD4 inhibitor Cl-amidine. Ex vivo treatment with Cl-amidine reduced the citrullinated histone H3/4 content in mouse neutrophils stimulated with the bacterial toxin ionomycin (Fig. 6*A*). In addition, incubation with Cl-amidine reduced the spontaneous and NOX-independent NETosis measured by the Sytox green staining of dsDNA released by cultured mouse neutrophils (Fig. 6*B*). PAD4 activity in the wound extract was increased in diabetic mice and reduced by pretreating mice with Cl-amidine (Fig. 6*C*). The circulating PAD4 activity was 10-fold lower compared with PAD4 activity in tissue (data not shown). PAD4 inhibition in the tissue reduced infiltrating NETting neutrophils, as shown by the decrease in Gr-1$^+$ Cit-H3/4$^+$ cells in the wound lysates of both diabetic and nondiabetic mice (Fig. 6*D* and *E*). Wound healing was delayed in mice with streptozotocin-induced diabetes compared with nondiabetic mice, whereas pretreatment with Cl-amidine restored the normal healing of diabetic wounds (Fig. 6*F*–*H*).

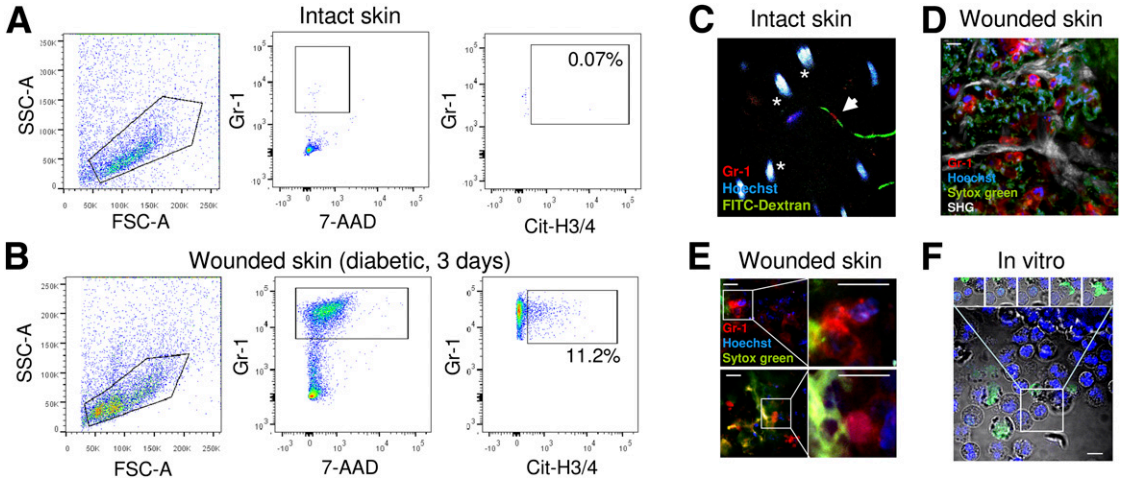

Figure 5—NETosis in mouse wound healing. *A*: A representative FACS plot showing that Gr-1$^+$ neutrophils are very rare in the tissue lysate of the intact unwounded skin and that a negligible fraction (<0.1%) is positive for the citrullinated H3/H4 histones. *B*: A representative FACS plot showing that Gr-1$^+$ neutrophils accumulate in the skin lysate of diabetic mice 3 days after wounding and that >10% are positive for the citrullinated H3/H4 histones and thereby undergoing NETosis. *C*: Intravital microscopy imaging of neutrophils and the vasculature in the intact skin. Gr-1$^+$ neutrophils (red, arrow) were almost never seen in the extravascular space and occasionally were detected while flowing through skin capillaries, stained in green with high–molecular weight fluorescein isothiocyanate (FITC)–conjugated dextran. *Autofluorescence of hair bulbs. *D*: Intravital microscopy imaging of Gr-1$^+$ neutrophils (red) infiltrating the wound bed 3 days after wounding. Nuclei are counterstained in blue with cell-permeable Hoechst 33342, whereas extracellular cell-free dsDNA is stained in green with the cell-impermeable Sytox green dye. The white signal of second harmonic generation (SHG) identifies collagen and blood vessels. The snapshot features a region of the wound bed rich in neutrophils, some of which show unlobulated nuclei or are devoid of nuclear staining, and extensive staining for extracellular dsDNA with Sytox green. *E*: Higher magnification details of the wound bed showing Gr-1$^+$ (red) neutrophils with decondensed chromatin and/or delobulated nuclei caught in the process of casting NETs, evidenced by the Sytox green staining in the close vicinity (areas in the inserts are magnified). *F*: Live in vitro recording of neutrophils labeled with Hoechst 33342 and stimulated with PMA, showing NETosis at different stages. Some neutrophils have intact lobulated nuclei with bright Hoechst 33342 signal and some have already undergone NET release (Sytox green in the medium stains extracellular dsDNA), whereas others are in the process of chromatin decondensation (low Hoechst 33342 staining intensity and nuclear delobulation). One of these is highlighted in the box, and the snapshots taken from Supplementary Video 1 show further nuclear decondensation and chromatin extrusion. Scale bar 10 μm from *C* to *F*. 7-AAD, 7-aminoactinomycin D; Cit-H3/4, citrullinated histones H3/H4; SSC-A, side scatter A; FSC-A, forward scatter A.

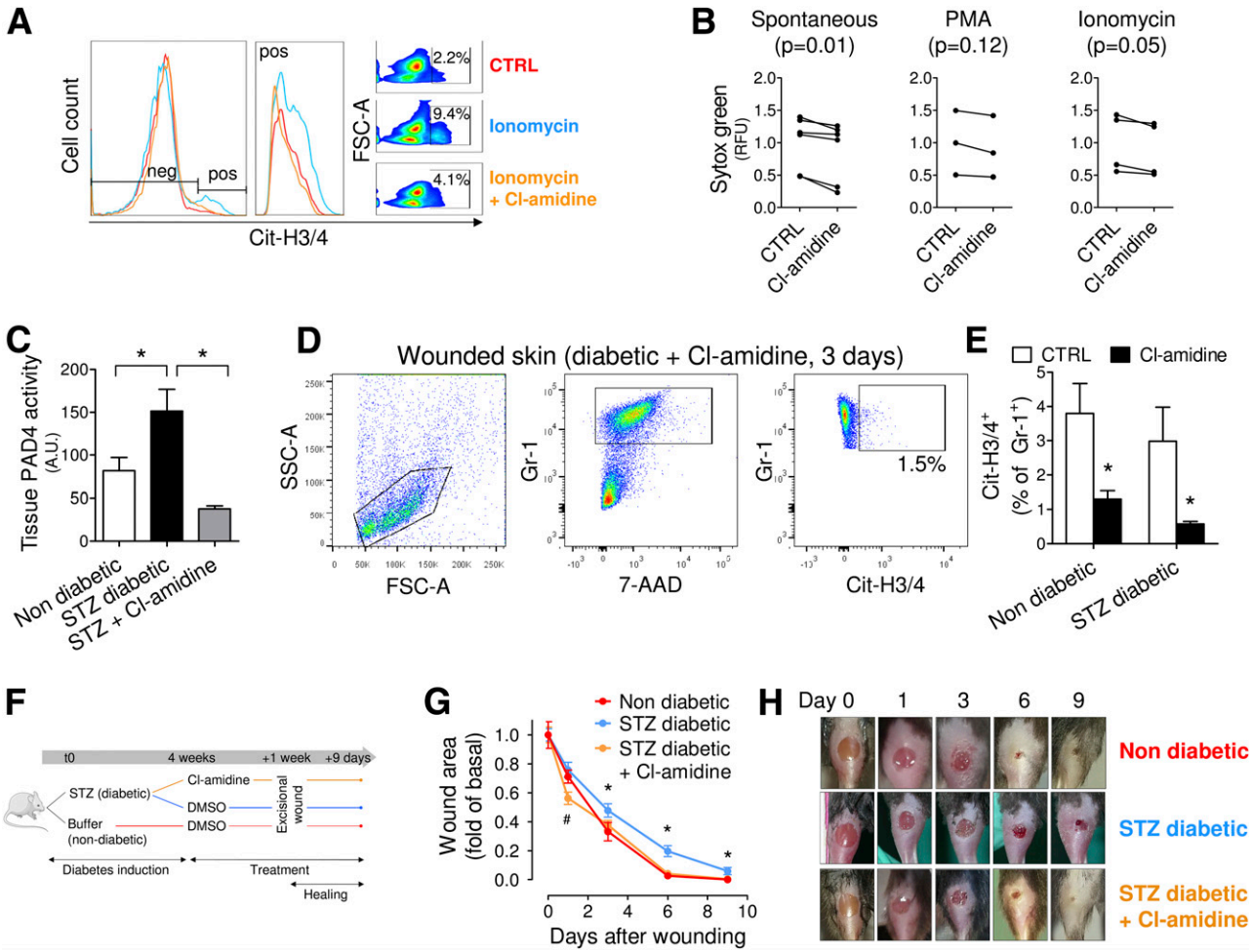

Figure 6—Inhibition of NETosis rescues wound healing in diabetic mice. *A*: Representative FACS staining for citrullinated histones H3/H4 (Cit-H3/4) of neutrophils stimulated with ionomycin with (orange) or without (blue) pretreatment with the PAD4 inhibitor Cl-amidine with respect to the control condition (red). Magnification of the positive events with mean fluorescence intensity as well as the respective populations and frequencies is shown. *B*: NET release by cultured neutrophils (evidenced by Sytox green staining of dsDNA in the medium) in the spontaneous condition, after PMA stimulation (NOX-dependent NETosis), or after ionomycin stimulation (NOX-independent NETosis) with or without (CTRL) PAD4 inhibition with Cl-amidine. *C*: PAD4 enzymatic activity in the tissue lysate of nondiabetic and streptozotocin (STZ) diabetic wounds, as well as in diabetic wounds from mice treated with Cl-amidine (*$P < 0.05$). *D*: Representative FACS plots showing reduction of citrullinated H3/H4$^+$ Gr-1$^+$ neutrophils in the skin lysate of diabetic mice treated with Cl-amidine. *E*: Quantification of citrullinated H3/H4$^+$ Gr-1$^+$ neutrophils in the wound lysate of diabetic and nondiabetic mice with and without (CTRL) PAD4 inhibition with Cl-amidine (*$P < 0.05$ vs. CTRL). *F*: Schematic representation of the wound healing experiment in nondiabetic and STZ diabetic with (Cl-amidine) and without (DMSO) pretreatment. *G*: Wound healing in nondiabetic, STZ diabetic, and diabetic mice treated with Cl-amidine as the fold change in wound area over time (*$P < 0.05$ for diabetic vs. nondiabetic; #$P < 0.05$ for Cl-amidine–treated vs. nondiabetic). *H*: Representative digital imaging of wounds from the 3 groups of mice up to day 9. neg, negative; pos, positive; RFU, relative fluorescence units; CTRL, subjects without diabetes; SSC-A, side scatter A; FSC-A, forward scatter A; A.U., arbitrary units; 7-AAD, 7-aminoactinomycin D.

DISCUSSION

This is the first study to show that an excess of NET proteins is associated with impaired wound healing and predicts a poor wound outcome in patients with diabetes. In addition, neutrophils isolated from patients with DFUs were prone to spontaneous NETosis but showed a defect in inducible NETosis. Consistently, data obtained in mice indicate that NETosis occurs in the wound bed and may causatively contribute to poor wound healing in subjects with diabetes. These findings suggest that NETosis inhibition is a potential therapeutic strategy for wound-healing acceleration in DFU patients.

NETosis is a physiological response to infection. The primary function of NETs is to entrap bacteria (6); however, increased NETosis promotes tissue damage and cytotoxic injury. NETosis-deficient PAD4$^{-/-}$ mice display a mildly impaired survival rate from polymicrobial sepsis; in addition, this mouse strain is protected from lipopolysaccharide-induced sterile shock (10). Therefore, a finely tuned balance of NETosis may be important to prevent sepsis while allowing for tissue repair. This balance is altered in diabetes and leads to impaired wound healing.

Two major types of NETosis have been described. Reactive oxygen species generated by NOX mediate the effect of PMA

(the most common NETosis inducer in vitro) and certain bacteria, such as *Pseudomonas aeruginosa* and *Escherichia coli* (20). NOX-independent NETosis has different signaling requirements (7), typically occurs in response to a *S. aureus* infection (21), and can be induced by calcium ionophores (e.g., ionomycin or a32187). We found that neutrophils from patients with DFUs had an enhanced spontaneous NETosis, concordant with elevated circulating NET-associated proteins, and an impaired NOX-independent NETosis. We speculate that diabetes biases neutrophil function from a defense to damage state by priming spontaneous NETosis and impairing a NETosis-mediated response to common infectious agents in DFU, such as *S. aureus*. Unlike dsDNA, the NET-associated enzymes elastase and proteinase-3 were higher in patients with infected wounds, especially wounds infected with Gram-positive bacteria. *S. aureus* DNase helps bacteria to escape the NETs, and extracellular dsDNA provides the majority of the antibacterial activity of NETs (22). Thus, NET enzymes alone would not be able to clear bacteria but would nonetheless damage the tissue (23).

Our previously generated and publically available proteomics data were reanalyzed for this study (14). Therefore, the findings in Fig. 1*A–D* that formed the basis for all of the subsequent analyses can be reproduced by other investigators. The NET components identified in NH wounds using a proteomic analysis (elastase, proteinase-3, NGAL, and histones) were found at higher concentrations in the blood of DFU patients. This systemic NET spreading may be the result of leakage from the wound tissue or production by circulating neutrophils. The latter hypothesis is supported by evidence that neutrophils isolated from the blood of DFU patients are primed for spontaneous NETosis. Therefore, these data identify a systemic component of DFUs that can potentially damage remote tissues and contribute to an overall poor prognosis.

In vitro, we visualized typical NETosis features using immunofluorescence and electron microscopy; however, these methods provide variable results (17). The release of elastase, MPO, and other granular proteins does not necessarily imply ongoing NETosis and may result from normal neutrophil degranulation. Thus, we quantified DNA-bound elastase and MPO from a bona fide NET fraction obtained by washing away unbound proteins and freeing NET proteins with S7 nuclease. This quantitative approach is more specific and insightful than the routine determination of elastase and dsDNA in the medium.

In vivo, our findings confirm and expand on the recent study by Wong et al. (13) that showed excess NETosis and delayed wound healing in diabetes may be due to PAD4 overexpression. Importantly, we used intravital microscopy to detect NETosis in the wound bed. This method allows for a reliable view of natural in vivo processes and is not subject to the biases of fixed-tissue imaging. Putative NETting cells were defined by the typical features observed during live recordings of NETosis in vitro; thus, these data provide a cross-validation of our observations. Furthermore, we pharmacologically inhibited PAD4 with Cl-amidine instead of using PAD4$^{-/-}$ mice and provided clinically transferrable evidence that NETosis machinery inhibition facilitates wound healing.

In conclusion, this study in mice and humans strongly expands our knowledge of the role of NETosis in one of the most threatening diabetes complications. These findings show that NETosis is detrimental for wound healing in subjects with diabetes; thus, therapeutic strategies aimed at modulating NETosis should be pursued to improve the outcome of DFU patients.

Acknowledgments. The authors acknowledge the editorial assistance of Kenneth Dyar (Institute for Diabetes and Obesity, HelmholtzZentrum München) and the technical assistance of Mario Bortolozzi and Filippo Romanato (Department of Physics and Astronomy "G. Galilei," University of Padova) for intravital microscopy.

Funding and Duality of Interest. The authors thank the "Cassa di Risparmio di Padova e Rovigo" (Cariparo) holding and "Veneto Banca" holding for funding the acquisition of the LTQ-Orbitrap-XL and MALDI-TOF/TOF mass spectrometers. G.P.F. is supported by grants from the Italian Ministry of Health (GR-2010-2301676 and GR-2011-02347600) and from a European Foundation for the Study of Diabetes/Novartis grant 2013 on microvascular complications. The study was also supported by a grant from the University of Padova, 2011 Strategic Project DYCENDI grant to F.M. and A.A., and by a grant from the Italian Ministry of Health (RF-2013-02358024) to M.A. No other potential conflicts of interest relevant to this article were reported.

Author Contributions. G.P.F. designed the study, researched and analyzed data, and wrote the manuscript. L.M., N.P., V.S., A.B., S.C., C.D.C., E.B., M.C.M., R.C., S.V.d.K., and M.A. researched and analyzed data. M.R. designed the study and researched data. F.M., G.A., and R.M. designed the study and researched and analyzed data. A.A. reviewed and edited the manuscript and contributed to discussion. All authors approved the final version of the manuscript. G.P.F. is the guarantor of this work and, as such, had full access to all the data in the study and takes responsibility for the integrity of the data and the accuracy of the data analysis.

References

1. Ramsey SD, Newton K, Blough D, et al. Incidence, outcomes, and cost of foot ulcers in patients with diabetes. Diabetes Care 1999;22:382–387

2. Brem H, Tomic-Canic M. Cellular and molecular basis of wound healing in diabetes. J Clin Invest 2007;117:1219–1222

3. Martin P, Leibovich SJ. Inflammatory cells during wound repair: the good, the bad and the ugly. Trends Cell Biol 2005;15:599–607

4. Dovi JV, He LK, DiPietro LA. Accelerated wound closure in neutrophil-depleted mice. J Leukoc Biol 2003;73:448–455

5. Remijsen Q, Kuijpers TW, Wirawan E, Lippens S, Vandenabeele P, Vanden Berghe T. Dying for a cause: NETosis, mechanisms behind an antimicrobial cell death modality. Cell Death Differ 2011;18:581–588

6. Brinkmann V, Reichard U, Goosmann C, et al. Neutrophil extracellular traps kill bacteria. Science 2004;303:1532–1535

7. Douda DN, Khan MA, Grasemann H, Palaniyar N. SK3 channel and mitochondrial ROS mediate NADPH oxidase-independent NETosis induced by calcium influx. Proc Natl Acad Sci U S A 2015;112:2817–2822

8. Leshner M, Wang S, Lewis C, et al. PAD4 mediated histone hypercitrullination induces heterochromatin decondensation and chromatin unfolding to form neutrophil extracellular trap-like structures. Front Immunol 2012;3:307

9. Villanueva E, Yalavarthi S, Berthier CC, et al. Netting neutrophils induce endothelial damage, infiltrate tissues, and expose immunostimulatory molecules in systemic lupus erythematosus. J Immunol 2011;187:538–552

10. Martinod K, Fuchs TA, Zitomersky NL, et al. PAD4-deficiency does not affect bacteremia in polymicrobial sepsis and ameliorates endotoxemic shock. Blood 2015;125:1948–1956

11. Menegazzo L, Ciciliot S, Poncina N, et al. NETosis is induced by high glucose and associated with type 2 diabetes. Acta Diabetol 2015;52: 497–503
12. Fadini GP, Menegazzo L, Scattolini V, Gintoli M, Albiero M, Avogaro A. A perspective on NETosis in diabetes and cardiometabolic disorders. Nutr Metab Cardiovasc Dis 2016;26:1–8
13. Wong SL, Demers M, Martinod K, et al. Diabetes primes neutrophils to undergo NETosis, which impairs wound healing. Nat Med 2015;21:815–819
14. Fadini GP, Albiero M, Millioni R, et al. The molecular signature of impaired diabetic wound healing identifies serpinB3 as a healing biomarker. Diabetologia 2014;57:1947–1956
15. Schaper NC. Diabetic foot ulcer classification system for research purposes: a progress report on criteria for including patients in research studies. Diabetes Metab Res Rev 2004;20(Suppl. 1):S90–S95
16. Lavery LA, Armstrong DG, Harkless LB. Classification of diabetic foot wounds. J Foot Ankle Surg 1996;35:528–531
17. Brinkmann V, Goosmann C, Kühn LI, Zychlinsky A. Automatic quantification of in vitro NET formation. Front Immunol 2012;3:413
18. Swamydas M, Lionakis MS. Isolation, purification and labeling of mouse bone marrow neutrophils for functional studies and adoptive transfer experiments. J Vis Exp 2013;77:e50586
19. Spengler J, Lugonja B, Ytterberg AJ, et al. Release of active peptidyl arginine deiminases by neutrophils can explain production of extracellular citrullinated autoantigens in RA synovial fluid. Arthritis Rheumatol 2015:67:3135–3145
20. Parker H, Dragunow M, Hampton MB, Kettle AJ, Winterbourn CC. Requirements for NADPH oxidase and myeloperoxidase in neutrophil extracellular trap formation differ depending on the stimulus. J Leukoc Biol 2012;92:841–849
21. Pilsczek FH, Salina D, Poon KK, et al. A novel mechanism of rapid nuclear neutrophil extracellular trap formation in response to Staphylococcus aureus. J Immunol 2010;185:7413–7425
22. Halverson TW, Wilton M, Poon KK, Petri B, Lewenza S. DNA is an antimicrobial component of neutrophil extracellular traps. PLoS Pathog 2015;11:e1004593
23. Herrick S, Ashcroft G, Ireland G, Horan M, McCollum C, Ferguson M. Up-regulation of elastase in acute wounds of healthy aged humans and chronic venous leg ulcers are associated with matrix degradation. Lab Invest 1997;77: 281–288